IMA Journal of Applied Mathematics (2013) **78**, 287–306
doi:10.1093/imamat/hxr050
Advance Access publication on November 17, 2011

Hopf bifurcation and Turing instability in the reaction–diffusion Holling–Tanner predator–prey model

XIN LI AND WEIHUA JIANG*
Department of Mathematics, Harbin Institute of Technology, Harbin, Heilongjiang 150001, People's Republic of China
*Corresponding author: jiangwh@hit.edu.cn

AND

JUNPING SHI
Department of Mathematics, College of William and Mary, Williamsburg, VA 23187-8795, USA

[Received on 10 January 2011; revised on 9 July 2011; accepted on 6 August 2011]

The reaction–diffusion Holling–Tanner predator–prey model with Neumann boundary condition is considered. We perform a detailed stability and Hopf bifurcation analysis and derive conditions for determining the direction of bifurcation and the stability of the bifurcating periodic solution. For partial differential equation (PDE), we consider the Turing instability of the equilibrium solutions and the bifurcating periodic solutions. Through both theoretical analysis and numerical simulations, we show the bistability of a stable equilibrium solution and a stable periodic solution for ordinary differential equation and the phenomenon that a periodic solution becomes Turing unstable for PDE.

Keywords: Hopf bifurcation; Turing instability; reaction–diffusion model; prey–predator system; Holling type-II functional response.

1. Introduction

We consider the following Holling–Tanner prey–predator model (May, 1973; Yi *et al.*, 2008)

$$\begin{aligned}\frac{\mathrm{d}H}{\mathrm{d}\tau} &= \upsilon H\left(1-\frac{H}{K}\right)-\frac{kHP}{H+D},\\ \frac{\mathrm{d}P}{\mathrm{d}\tau} &= sP\left(1-\frac{cP}{H}\right),\end{aligned} \tag{1.1}$$

where υ and s are the intrinsic growth rates of the prey (H) and predator (P) populations, respectively. The *per capita* growth rate of the prey is of the common logistic form, and K is the carrying capacity, the maximum number of the prey allowed by the limited resource. The predation function is represented by a Holling type-II function which is extensively used in invertebrate ecology. The constant k is the maximum of the predation rate when the predator will not or cannot kill more prey even when the latter is available. The constant D refers to some value of the prey population beyond which the predators attacking capability begins to saturate. The predator population also grows in logistic form, and c is the number of preys required to support one predator at equilibrium, when P equals H/c (Tanner, 1975).

We consider the two populations in a spatial domain $r \in (0,\pi)$, and we use $x(r,t)$ and $y(r,t)$ to denote the population densities of the prey and the predator, respectively. The dispersal of species in the spatial domain is assumed to be random, so that Fick's law holds, and it leads to the well-known diffusion equations as follows:

$$\frac{\partial x}{\partial \tau} = d_1 \frac{\partial^2 x}{\partial r^2}, \quad \frac{\partial y}{\partial \tau} = d_2 \frac{\partial^2 y}{\partial r^2},$$

where d_i $(i = 1, 2)$ are the diffusion coefficients. With the addition of diffusion and non-dimensionalization, the system (1.1) becomes

$$\begin{cases} \dfrac{\partial x}{\partial t} = d_1 \dfrac{\partial^2 x}{\partial r^2} + x(1 - \beta x) - \dfrac{my}{x+1}, & r \in (0, \pi), \quad t > 0, \\ \dfrac{\partial y}{\partial t} = d_2 \dfrac{\partial^2 y}{\partial r^2} + sy\left(1 - \dfrac{y}{x}\right), & r \in (0, \pi), \quad t > 0, \end{cases} \tag{1.2}$$

where $t = \upsilon\tau$, $x = H/D$, $y = cP/D$, $m = k/(\upsilon c)$ and $\beta = D/K$. We assume the no-flux boundary conditions so the ecosystem is a closed one:

$$\frac{\partial x(0,t)}{\partial r} = \frac{\partial x(\pi,t)}{\partial r} = \frac{\partial y(0,t)}{\partial r} = \frac{\partial y(\pi,t)}{\partial r} = 0.$$

The system (1.1) was first studied by Tanner (1975), and he showed that under certain conditions the relative sizes of growth rates could determine the stability of the system and stated a hypothesis for the conclusion that either a stable prey population possesses strong self-limitation or the growth rate of the prey species is less than that of its predator. He tested his hypothesis by estimating the intrinsic growth rates for certain prey species and their predators. In his book, Murray (2002) studied the stability of the positive equilibrium and the existence of the limit cycles of system (1.1). Hsu & Huang (1995) dealt with the question of global stability of the positive equilibrium in a class of predator–prey systems including system (1.1) with certain conditions on the parameters, applying Dulac's criterion and Lyapunov functions construction. In Hsu & Huang (1998), they proved the uniqueness of limit cycle when the unique positive equilibrium is unstable. In Hsu & Huang (1999), they showed that for some parameter range the Hopf bifurcation of system (1.1) is subcritical, i.e., near the Hopf bifurcation point, there exists a small-amplitude repelling periodic orbit enclosing a stable equilibrium and there are multiple limit cycles. Gasull *et al.* (1997) gave a negative answer to the question: does the asymptotic stability of the positive equilibrium of the system (1.1) imply the global stability? They computed the Poincaré–Lyapunov constants in case a weak focus occurs, and in this way they were able to construct an example with two limit cycles.

For the partial differential equation (PDE) model, Du & Hsu (2004) considered a diffusive Leslie–Gower predator–prey model, which was a special case of system (1.2), but in a heterogeneous environment. They showed that positive steady-state solutions with certain prescribed spatial patterns can be obtained if the coefficient functions are chosen suitably and observed some essential differences in the behaviour of their model from that of the Lotka–Volterra model that seemed to arise only in the heterogeneous case. Peng & Wang (2005) studied system (1.2), and they obtained the existence and non-existence of positive non-constant steady states. In Peng & Wang (2007), they obtained some results for the global stability of the unique positive equilibrium of system (1.2). Recently, Chen *et al.* (2010) considered a diffusive Leslie–Gower predator–prey model with delay, and they proved the global stability of constant equilibrium even with delay effect, which improved an earlier result of Du & Hsu (2004).

For the studies of Hopf bifurcation for reaction–diffusion (R-D) system, Yi *et al.* (2009a) derived an explicit algorithm for determining the direction of Hopf bifurcation and stability of the bifurcating periodic solutions for an R-D system consisting of two equations with Neumann boundary condition. In particular, they have shown the existence of multiple spatially non-homogeneous periodic orbits while the system parameters are all spatially homogeneous. Earlier, Yi *et al.* (2008) considered a Lengyel–Epstein R-D system of the chlorite–iodide–malonic acid reaction, and they derived the precise conditions on the parameters so that the spatially homogeneous equilibrium solution and the spatially homogeneous periodic solution become Turing unstable. They also studied the global asymptotical behaviour of the Lengyel–Epstein R-D system in Yi *et al.* (2009b). Similar work along this line has been done recently for Gierer–Meinhardt model (Liu *et al.*, 2010; Ruan, 1998), Sel'kov model (Han & Bao, 2009) and a biomolecular model with autocatalysis and saturation law (Yi *et al.*, 2010). See also Shi (2009) for a recent survey on abstract bifurcation theorems and applications to spatiotemporal models from ecology and biochemistry.

In this article, we analyse the stability and Hopf bifurcation of the positive equilibrium in both ordinary differential equation (ODE) and PDE models and derive conditions for determining the direction of bifurcation and the stability of the bifurcating periodic solution. For PDE, we also derive the precise conditions on the parameters so that the spatially homogeneous equilibrium solution and the spatially homogeneous periodic solution become Turing unstable. By both theoretical analysis and numerical simulations, we show the coexistence of a stable equilibrium point, an unstable limit cycle and a stable limit cycle for ODE and a Turing unstable periodic solution is attracted by a stable non-constant steady state for PDE. The latter result confirms the results obtained in Peng & Wang (2005).

The rest of this article is organized as follows: In Section 2, we investigate the asymptotical behaviour of the equilibrium and occurrence of Hopf bifurcation of the local system (the ODE model). In Section 3, we consider the diffusion-driven instability of the equilibrium solution. In Section 4, we analyse the stability of the bifurcating periodic solution, which is a spatially homogeneous periodic solution of the R-D system, through the Hopf bifurcation when the spatial domain is a bounded interval. In Section 5, we carry out some numerical simulations to illustrate the analytical results. In Section 6, we end our investigation with concluding remarks, and we summarize our result in a bifurcation diagram.

2. Analysis of the local system

For system (1.2), the local system is an ODE in the form of

$$\begin{cases} \dfrac{\mathrm{d}x}{\mathrm{d}t} = x(1-\beta x) - \dfrac{mxy}{x+1} := f(x,y), \\ \dfrac{\mathrm{d}y}{\mathrm{d}t} = sy\left(1-\dfrac{y}{x}\right) := g(x,y), \\ x(0) > 0, \quad y(0) > 0. \end{cases} \tag{2.1}$$

The non-dimensional form which we use here is different from the ones used in previous papers. By using this form, we can deal with the stability of the equilibrium solutions in an easier way.

System (2.1) has two non-trivial equilibrium points, a boundary equilibrium point $E_1 \equiv (1/\beta, 0)$ and a positive equilibrium point $E_2 \equiv (x^*, y^*)$, where

$$x^* = y^* = \frac{1}{2\beta}\left(\sqrt{R^2+4\beta} - R\right), \quad R = \beta + m - 1.$$

By simple calculations, we know that the boundary equilibrium E_1 is a saddle point with the positive x-axis as its stable manifold. We are interested in studying the properties of the positive equilibrium

$E_2 \equiv (x^*, y^*)$. Before considering the stability of E_2, we present the following result, which states that system (2.1) is as 'well behaved' as one intuits from the biological problem. A corresponding result for a different non-dimensional form is presented in Hsu & Huang (1995) without proof.

LEMMA 2.1 The solutions of system (2.1) are positive and eventually bounded, i.e., there exists $T \geqslant 0$ such that $x(t) < 1/\beta$, $y(t) < 1/\beta$ for $t \geqslant T$.

Proof. The phase portrait of (2.1) is shown in Fig. 1. The nullclines of the systems are: C_1: $y = \frac{1}{m}(1-\beta x)(1+x)$, on which $\mathrm{d}x/\mathrm{d}t = 0$; and C_2: $y = x$, on which $\mathrm{d}y/\mathrm{d}t = 0$. The first quadrant is divided into four parts D_1, D_2, D_3 and D_4 by C_1 and C_2. The intersection of C_1 and C_2 is the positive equilibrium point (x^*, y^*). Set $L_1 = \{(x, y): x = 1/\beta,\ 0 \leqslant y \leqslant 1/\beta\}$ and $L_2 = \{(x, y): 0 \leqslant x \leqslant 1/\beta,\ y = 1/\beta\}$. Denote $\mathscr{D}$ as the rectangular region whose boundary consists of L_1, L_2, x-axis and y-axis. It is clear that $\mathscr{D}$ is an invariant set and attracts any trajectory starting in the first quadrant. Hence, the solutions are eventually bounded.

Next we prove the positivity of the solutions by showing that trajectories starting from the first quadrant cannot reach the y-axis. To this end we only need to prove that trajectories cannot arrive the y-axis in D_2.

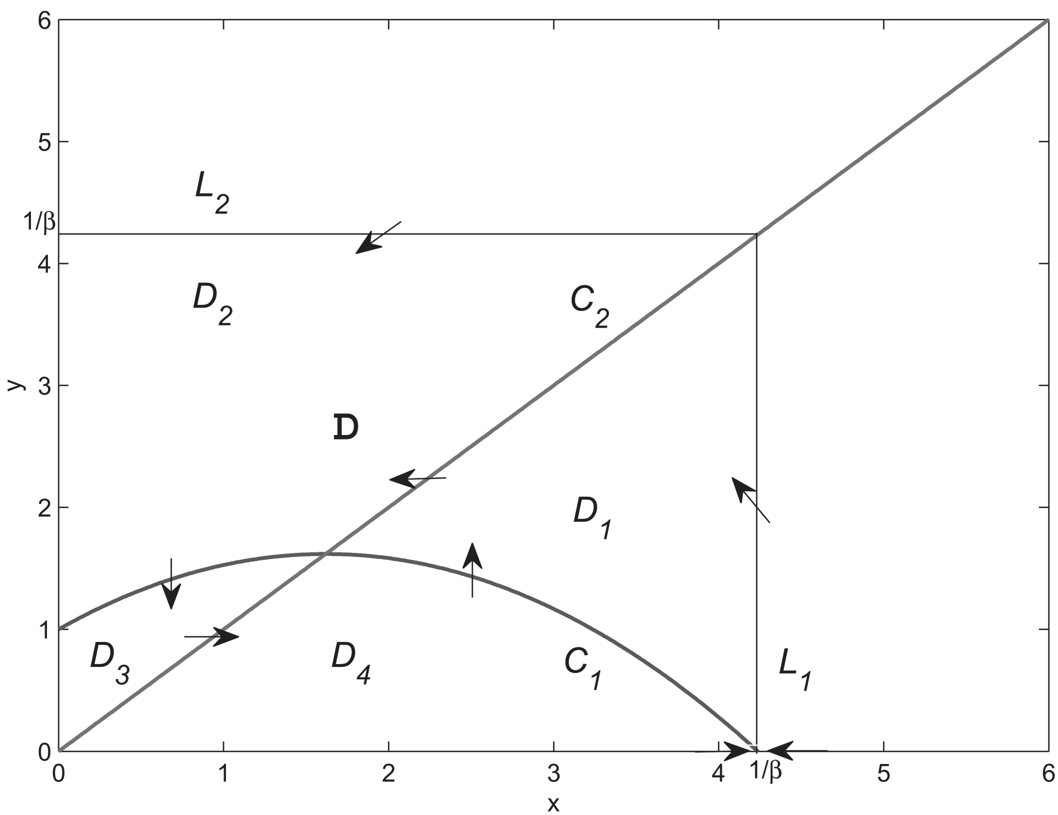

FIG. 1. Phase portrait of (2.1) in xy-plane.

For a given point $(x_0, y_0) \in D_2$, denote T_1 as the time of the trajectory running from (x_0, y_0) to C_1 and $T_2(N)$ as the time of the trajectory running from (x_0, y_0) to the line $x = x_0/N$, $N \in \mathbb{N}$ and $N \geqslant 2$. We estimate the time T_1 and T_2.

$$T_1 \leqslant \int_{y_0}^{1} \frac{1}{sy\left(1-\frac{y}{x}\right)} \mathrm{d}y \leqslant \int_{1}^{y_0} \frac{1}{sy\left(\frac{y}{x_0}-1\right)} \mathrm{d}y = \frac{1}{s} \ln\left(\frac{1-\frac{x_0}{y_0}}{1-x_0}\right).$$

It is clear that T_1 is finite. While

$$T_2(N) = \int_{x_0}^{\frac{x_0}{N}} \frac{1}{x(1-\beta x) - \frac{mxy}{x+1}} \mathrm{d}x \quad \geqslant \int_{x_0}^{\frac{x_0}{N}} \frac{1}{x(\beta x + my_0 - 1)} \mathrm{d}x$$

$$= \frac{1}{my_0 - 1} \ln\left(\frac{\beta x_0 + N(my_0 - 1)}{\beta x_0 + my_0 - 1}\right),$$

since

$$\lim_{N\to+\infty} \frac{1}{my_0 - 1} \ln\left(\frac{\beta x_0 + N(my_0 - 1)}{\beta x_0 + my_0 - 1}\right) = +\infty,$$

there exists an $N_0 \in \mathbb{N}$ such that

$$\frac{1}{my_0 - 1} \ln\left(\frac{\beta x_0 + N_0(my_0 - 1)}{\beta x_0 + my_0 - 1}\right) > \frac{1}{s} \ln\left(\frac{1-\frac{x_0}{y_0}}{1-x_0}\right),$$

hence, $T_2(N_0) > T_1$. This shows that the time of the trajectory running to the y-axis is far longer than that to C_1, that is the trajectory runs into D_3 before it reaches the y-axis. From the properties of the vector field shown in Fig. 1, the trajectories cannot reach the y-axis in D_3, so any trajectories starting in the first quadrant cannot reach the y-axis.

From the above discussion, we know that there is no homoclinic or heteroclinic orbit in the domain $\mathscr{D}$. Then the conclusion is proved. □

Now we study the stability of E_2. The Jacobian matrix of system (2.1) at (x^*, y^*) is

$$J(s) := \begin{pmatrix} s_0 & b \\ s & -s \end{pmatrix},$$

where $s_0 = 1 - 2\beta x^* - \dfrac{my^*}{(1+x^*)^2}$, $b = -\dfrac{mx^*}{1+x^*}$. The characteristic equation corresponding to E_2 is

$$\lambda^2 - (s_0 - s)\lambda - s(s_0 + b) = 0. \tag{2.2}$$

Note that $s_0 + b = -\dfrac{1+\beta x^{*2}}{1+x^*} < 0$, where we use the fact that $y^* = \dfrac{1}{m}(1-\beta x^*)(1+x^*)$. So all roots of (2.2) have negative real parts if and only if $s > s_0$. Now we consider the following two cases: $s_0 > 0$ and $s_0 \leqslant 0$. Note that $s_0 = \dfrac{x^*}{1+x^*}\left(m - \sqrt{R^2 + 4\beta}\right)$, so $s_0 > 0$ if and only if

$$(\mathrm{H}_1) \quad \beta < 1 \text{ and } m > \frac{(1+\beta)^2}{2(1-\beta)},$$

$s_0 \leqslant 0$ if and only if

$$(\mathrm{H}_1') \quad \beta \geqslant 1, \quad \text{or } \beta < 1 \text{ and } m \leqslant \frac{(1+\beta)^2}{2(1-\beta)}.$$

When (H_1') holds, we always have $s > 0 \geqslant s_0$, so E_2 is locally asymptotically stable. Furthermore, we state the global stability of E_2 in the following result.

THEOREM 2.1 Suppose that $\beta, m, s > 0$.

1. If (H_1') holds, then (x^*, y^*) is globally asymptotically stable;
2. If (H_1) holds and $s > s_0$, then (x^*, y^*) is locally asymptotically stable;
3. If (H_1) holds and $s < s_0$, then (x^*, y^*) is unstable and there exists at least one periodic orbit for (2.1).

Proof. Part 2 from the analysis given above. Part 1 follows from Theorem 2.2 in Hsu & Huang (1995). Part 3 is from Lemma 2.1 and the Poincaré–Bendixson Theorem. Suppose (H_1') holds, we have

$$(x - x^*)\left(\frac{1}{m}(1-\beta x)(1+x) - y^*\right) < 0 \ \text{ for } \ x > 0, \ x \neq x^*.$$

□

Next we analyse the Hopf bifurcation occurring at (x^*, y^*). Since the equilibrium point (x^*, y^*) is globally asymptotically stable when (H_1') holds, we always assume that β and m are fixed so that (H_1) holds in the following, and we use s as the bifurcation parameter. When s is near s_0, the characteristic equation (2.2) has a pair of complex roots $\lambda(s) = \alpha(s) \pm i\omega(s)$, where $\alpha(s) = \frac{1}{2}(s_0 - s)$, $\omega(s) = \frac{1}{2}\sqrt{-4bs - (s_0+s)^2}$ and $\alpha(s_0) = 0$, $\alpha'(s_0) = -1/2 < 0$.

By the Poincaré–Andronov–Hopf Bifurcation Theorem, we know that system (2.1) undergoes a Hopf bifurcation at (x^*, y^*) when $s = s_0$. However, the detailed property of the Hopf bifurcation needs further analysis of the normal form. To that end we transform the equilibrium (x^*, y^*) to the origin by the transformation $\tilde{x} = x - x^*$ and $\tilde{y} = y - y^*$. For convenience, we still denote $\tilde{x}$ and $\tilde{y}$ by x and y, respectively. Thus, the local system becomes

$$\begin{pmatrix} \dfrac{\mathrm{d}x}{\mathrm{d}t} \\[2mm] \dfrac{\mathrm{d}y}{\mathrm{d}t} \end{pmatrix} = J(s)\begin{pmatrix} x \\ y \end{pmatrix} + \begin{pmatrix} f_1(x, y, s) \\ f_2(x, y, s) \end{pmatrix}. \tag{2.3}$$

Here

$$f_1(x, y, s) = A_{20}x^2 + A_{11}xy + A_{30}x^3 + A_{21}x^2y + \mathcal{O}(|x|^4, |x|^3|y|),$$

$$f_2(x, y, s) = B_{20}x^2 + B_{11}xy + B_{02}y^2 + B_{30}x^3 + B_{21}x^2y + B_{12}xy^2 + \mathcal{O}(|x|^4, |x|^3|y|, |x|^2|y|^2),$$

where

$$A_{20} := \frac{1 - \beta x^* - \beta(1+x^*)^2}{(1+x^*)^2}, \ A_{11} := -\frac{m}{(1+x^*)^2}, \ A_{30} := \frac{\beta x^* - 1}{(1+x^*)^3}, \ A_{21} := \frac{m}{(1+x^*)^3},$$

$$B_{20} := -\frac{s}{x^*},\ B_{11} := \frac{2s}{x^*},\ B_{02} := -\frac{s}{x^*},\ B_{30} := \frac{s}{x^{*2}},\ B_{21} := -\frac{2s}{x^{*2}},\ B_{12} := \frac{s}{x^{*2}}.$$

Set matrix

$$T := \begin{pmatrix} N & 1 \\ M & 0 \end{pmatrix},$$

then

$$T^{-1}J(s)T = \Lambda(s) := \begin{pmatrix} \alpha(s) & -\omega(s) \\ \omega(s) & \alpha(s) \end{pmatrix},$$

where $M = -\frac{s}{\omega}$ and $N = -\frac{s_0+s}{2\omega}$. Via the transformation $(x, y)^\top = T(u, v)^\top$, system (2.1) becomes

$$\begin{pmatrix} \frac{\mathrm{d}u}{\mathrm{d}t} \\ \frac{\mathrm{d}v}{\mathrm{d}t} \end{pmatrix} = \Lambda(s)\begin{pmatrix} u \\ v \end{pmatrix} + \begin{pmatrix} F^1 \\ F^2 \end{pmatrix}, \tag{2.4}$$

where

$$\begin{pmatrix} F^1 \\ F^2 \end{pmatrix} := T^{-1}\begin{pmatrix} f_1(Nu+v, Mu) \\ f_2(Nu+v, Mu) \end{pmatrix} = \begin{pmatrix} \frac{1}{M} f_2(Nu+v, Mu) \\ f_1 - \frac{N}{M} f_2(Nu+v, Mu) \end{pmatrix}.$$

Rewrite (2.4) in the following polar coordinates form:

$$\begin{aligned} \dot{r} &= \alpha(s)r + a(s)r^3 + \cdots, \\ \dot{\theta} &= \omega(s) + c(s)r^2 + \cdots, \end{aligned} \tag{2.5}$$

then the Taylor expansion of (2.4) at $s = s_0$ yields

$$\begin{aligned} \dot{r} &= \alpha'(s_0)(s-s_0)r + a(s_0)r^3 + \mathcal{O}((s-s_0)^2 r,\ (s-s_0)r^3,\ r^5), \\ \dot{\theta} &= \omega(s_0) + \omega'(s_0)(s-s_0) + c(s_0)r^2 + \mathcal{O}((s-s_0)^2,\ (s-s_0)r^2,\ r^4). \end{aligned} \tag{2.6}$$

In order to determine the stability of the periodic solution, we need to calculate the sign of the coefficient $a(s_0)$, which is given by

$$\begin{aligned} a(s_0) :=& \frac{1}{16}[F^1_{uuu} + F^1_{uvv} + F^2_{uuv} + F^2_{vvv}] \\ &+ \frac{1}{16\omega(s_0)}[F^1_{uv}(F^1_{uu} + F^1_{vv}) - F^2_{uv}(F^2_{uu} + F^2_{vv}) - F^1_{uu}F^2_{uu} + F^1_{vv}F^2_{vv}], \end{aligned}$$

where all partial derivatives are evaluated at the bifurcation point $(x, y, s) = (0, 0, s_0)$. The explicit calculation of the coefficient $a(s_0)$ can be found in Guckenheimer & Holmes (1983), Hassard *et al.* (1980), Marsden & McCracken (1976) and Wiggins (1990). Thus, we can calculate that

$$
\begin{aligned}
a(s_0) =& \frac{1}{8}[(3A_{30} + 2A_{21})N_0^2 + 3A_{30} - 2B_{12}] \\
& - \frac{1}{8\omega_0}\Big[(2A_{20} + A_{11})(A_{20} + A_{11})N_0^3 + (2A_{20} + A_{11})(A_{20} - B_{20})N_0 \\
& \qquad -2B_{20}(A_{20} - B_{20})\frac{1}{N_0}\Big],
\end{aligned}
$$

where $N_0 := N|_{s=s_0} = -\sqrt{-\dfrac{s_0}{s_0+b}}$ and $\omega_0 := \omega(s_0) = \sqrt{-s_0(s_0+b)}$. Clearly, we can regard $a(s_0)$ as a function about β and m. The expression of $a(s_0)$ by β and m is cumbersome to present here, thus we omit it. But $a(s_0) = 0$ defines a curve in the βm-plane. With the symbolic mathematical software `Matlab`, we plot the curve $a(s_0) = 0$ in the βm-plane, together with the curve $m = \dfrac{(1+\beta)^2}{2(1-\beta)}$ in Fig. 2.

Now from Poincaré–Andronov–Hopf Bifurcation Theorem, $\alpha'(s)|_{s=s_0} = -1/2 < 0$ and the above calculation of $a(s_0)$, we summarize our results.

THEOREM 2.2 Suppose that (H_1) holds, and let $s_0 = \dfrac{\sqrt{R^2+4\beta} - R}{2\beta + \sqrt{R^2+4\beta} - R}(m - \sqrt{R^2+4\beta})$ where $R = \beta + m - 1$.

1. The coexistence equilibrium (x^*, y^*) of system (2.1) is locally asymptotically stable when $s > s_0$ and is unstable when $s < s_0$.
2. System (2.1) undergoes a Hopf bifurcation at (x^*, y^*) when $s = s_0$. When $a(s_0) < 0$, the direction of the Hopf bifurcation is supercritical and the bifurcating periodic solutions are orbitally asymptotically stable; when $a(s_0) > 0$, the direction of the Hopf bifurcation is subcritical and the bifurcating periodic solutions are unstable.

The phenomenon of bifurcation for model (1.1) shown by Theorem 2.2 coincide with that in Gasull *et al.* (1997) and Hsu & Huang (1999). We have the following result directly from Theorem 2.2 and Poincaré–Bendixson Theorem.

COROLLARY 2.1 Under the assumption in Theorem 2.2, when $a(s_0) > 0$ and $s \in (s_0, s_0 + \epsilon)$, there exist at least two periodic orbits for system (2.1).

In Fig. 2, a subcritical Hopf bifurcation occurs if (β, m) is above the curve P_2, while a supercritical Hopf bifurcation occurs if (β, m) falls between the curve P_1 and P_2. For (β, m) below P_1, the global stability of (x^*, y^*) always holds. A corresponding result for a different non-dimensional form is presented in Gasull *et al.* (1997).

3. Turing instability of coexistence equilibrium

In 1953, Turing (1952) showed that, a system of coupled R-D equations can be used to describe patterns and forms in biological systems. Turing's theory shows that the interplay of chemical reaction and diffusion may cause the stable equilibrium of the local system to become unstable for the diffusive

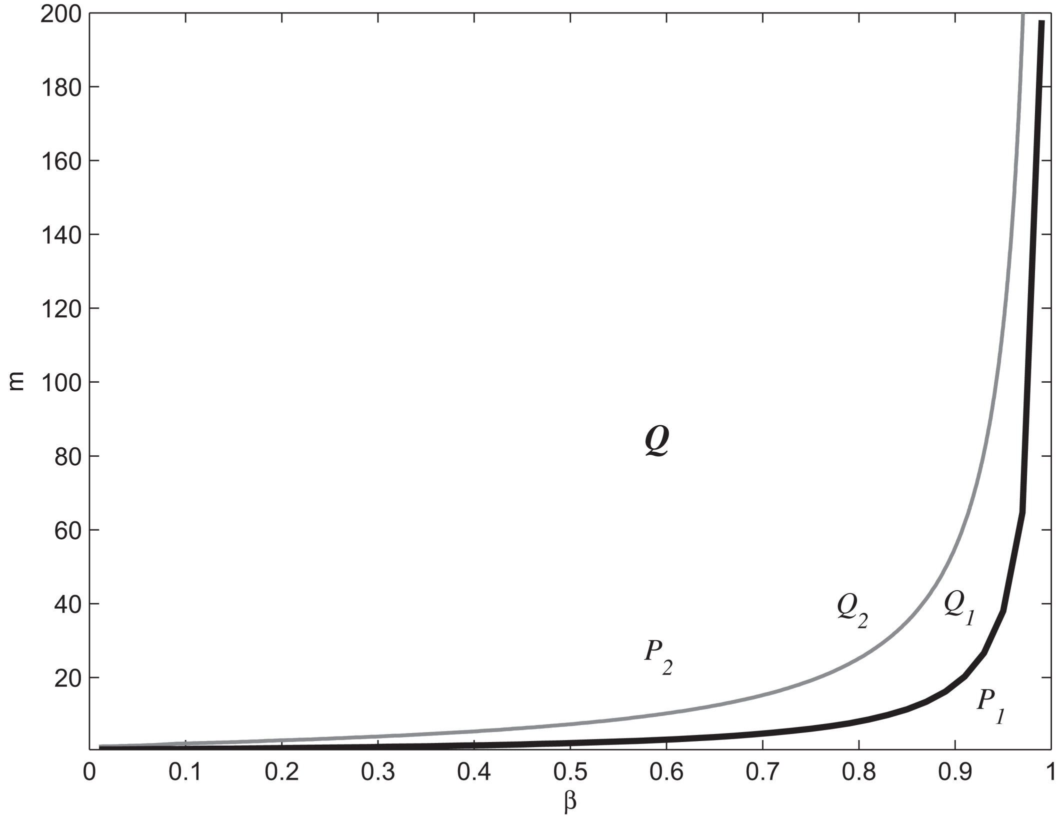

FIG. 2. Graph of $a(s_0) = 0$ on the condition (H_1). The curve $P_1 = \left\{(\beta, m)|\ m = \frac{(1+\beta)^2}{2(1-\beta)},\ 0 < \beta < 1\right\}$, the curve $P_2 = \{(\beta, m)|\ a(s_0) = 0,\ 0 < \beta < 1\}$, the region $Q = \left\{(\beta, m)|\ m > \frac{(1+\beta)^2}{2(1-\beta)},\ 0 < \beta < 1\right\}$, which is divided by P_2 into two regions Q_1 where $a(s_0) < 0$ and Q_2 where $a(s_0) > 0$.

system and lead to the spontaneous formulation of a spatially periodic stationary structure. This kind of instability is called *Turing instability* or *diffusion-driven instability*.

In this part, we derive conditions for the Turing instability for the spatially homogeneous equilibrium solution of the R-D Holling–Tanner model. Here we consider the special case with the no-flux boundary condition in a one-dimensional interval $(0, \pi)$:

$$\begin{cases} \dfrac{\partial x}{\partial t} = d_1 \dfrac{\partial^2 x}{\partial r^2} + x(1 - \beta x) - \dfrac{mxy}{x+1}, & r \in (0, \pi),\quad t > 0, \\ \dfrac{\partial y}{\partial t} = d_2 \dfrac{\partial^2 y}{\partial r^2} + sy\left(1 - \dfrac{y}{x}\right), & r \in (0, \pi),\quad t > 0, \\ x_r(0, t) = x_r(\pi, t) = 0, & t > 0, \\ y_r(0, t) = y_r(\pi, t) = 0, & t > 0. \end{cases} \tag{3.1}$$

The operator $\phi \mapsto -\phi''$ on $(0, \pi)$ with boundary condition $\phi'(0) = \phi'(\pi) = 0$ has eigenvalues

$$\mu_0 = 0, \quad \mu_k = k^2, \quad k = 1,\ 2,\ 3, \ldots,$$

and normalized eigenfunctions

$$\phi_0(r) = \sqrt{\frac{1}{\pi}}, \quad \phi_k(r) = \sqrt{\frac{2}{\pi}} \cos(kr), \quad k = 1,\ 2,\ 3, \ldots.$$

The linearized system of (3.1) at (x^*, y^*) has the form:

$$\begin{pmatrix} x_t \\ y_t \end{pmatrix} = L(s) \begin{pmatrix} x \\ y \end{pmatrix} := D \begin{pmatrix} \Delta x \\ \Delta y \end{pmatrix} + J(s) \begin{pmatrix} x \\ y \end{pmatrix}, \tag{3.2}$$

where $J(s)$ is the Jacobian matrix defined in Section 2 and

$$D := \begin{pmatrix} d_1 & 0 \\ 0 & d_2 \end{pmatrix}.$$

$L(s)$ is a linear operator with domain $D_L = X_{\mathbb{C}} := X \oplus iX = \{x_1 + ix_2 : x_1, x_2 \in X\}$, where $X := \{(x, y) \in H^2[(0, \pi)] \times H^2[(0, \pi)] : x'(0) = x'(\pi) = y'(0) = y'(\pi) = 0\}$ is a real-valued Sobolev space.

Consider the following characteristic equation of the operator $L(s)$:

$$L(s) \begin{pmatrix} \phi \\ \psi \end{pmatrix} = \mu \begin{pmatrix} \phi \\ \psi \end{pmatrix}.$$

Let $(\phi(r), \psi(r))^\top$ be an eigenfunction of $L(s)$ corresponding to the eigenvalue μ, and let

$$\begin{pmatrix} \phi \\ \psi \end{pmatrix} = \sum_{k=0}^{\infty} \begin{pmatrix} a_k \\ b_k \end{pmatrix} \cos(kr),$$

where a_k and b_k are coefficients. We obtain that

$$-D \sum_{k=0}^{\infty} k^2 \begin{pmatrix} a_k \\ b_k \end{pmatrix} \cos kr + J(s) \sum_{k=0}^{\infty} \begin{pmatrix} a_k \\ b_k \end{pmatrix} \cos kr = \mu \sum_{k=0}^{\infty} \begin{pmatrix} a_k \\ b_k \end{pmatrix} \cos kr,$$

then

$$(J(s) - k^2 D) \begin{pmatrix} a_k \\ b_k \end{pmatrix} = \mu \begin{pmatrix} a_k \\ b_k \end{pmatrix}, \quad (k = 0,\ 1,\ 2, \ldots).$$

Denote

$$J_k := J(s) - k^2 D = \begin{pmatrix} s_0 - k^2 d_1 & b \\ s & -s - k^2 d_2 \end{pmatrix}, \quad (k = 0,\ 1,\ 2, \ldots).$$

It is clear that the eigenvalues of $L(s)$ are given by the eigenvalues of J_k for $k = 0, 1, 2, \ldots$. The characteristic equation of J_k is

$$\mu^2 - T_k\mu + D_k = 0, \quad k = 0,\ 1,\ 2, \ldots, \tag{3.3}$$

where

$$T_k := \operatorname{tr} J_k = s_0 - s - k^2(d_1 + d_2),$$

$$D_k := \det J_k = d_1 d_2 k^4 + (d_1 s - d_2 s_0)k^2 - s(s_0 + b).$$

By analysing the distribution of the roots of (3.3) , we can obtain the following conclusion.

THEOREM 3.1 Suppose that (H_1) holds and $s > s_0$, such that (x^*, y^*) is a locally asymptotically stable equilibrium for system (2.1). Then (x^*, y^*) is a locally asymptotically stable equilibrium solution of system (3.1) if and only if one of following is statisfied

(H_2) $d_1 \geqslant s_0$;

(H_3) $d_1 \geqslant \dfrac{d_2 s_0}{s}$;

(H_4) $d_1 < \min\left\{s_0, \dfrac{d_2 s_0}{s}\right\}$ and $s > \dfrac{d_2 k^2(s_0 - d_1 k^2)}{d_1 k^2 - (s_0 + b)}$, for all $k \geqslant 1$ satisfying $k < \sqrt{\dfrac{s_0}{d_1}}$,

and (x^*, y^*) is an unstable equilibrium solution of (3.1) if

(H_5) $d_1 < \min\left\{s_0, \dfrac{d_2 s_0}{s}\right\}$ and $s < \dfrac{d_2 K^2(s_0 - d_1 K^2)}{d_1 K^2 - (s_0 + b)}$, for some $K \in \mathbb{N}$ satisfying $K < \sqrt{\dfrac{s_0}{d_1}}$.

Thus, the equilibrium (x^*, y^*) is Turing unstable if s belongs to the interval:

$$I_K = \left\{s\colon\ s_0 < s < \frac{d_2 K^2(s_0 - d_1 K^2)}{d_1 K^2 - (s_0 + b)}\right\}.$$

That is, if $s \in I_K$, then (x^*, y^*) is locally asymptotically stable with respect to the ODE dynamics (2.1), and it is unstable with respect to the PDE (3.1).

Proof. First, it is clear that, $T_{k+1} < T_k$ for $k \geqslant 0$ from the definition of T_k, and $T_0 < 0$. So $T_k < 0$, for all $k \geqslant 0$. Hence, the signs of the real parts of roots of (3.3) are determined by the signs of D_k, respectively. We regard D_k as a quadratic function about k^2 denoted by $D(k^2)$, that is, $D(k^2) := d_1 d_2 k^4 + (d_1 s - d_2 s_0)k^2 - s(s_0 + b)$, $k \in \mathbb{N}$. The symmetry axis of the graph of $(k^2, D(k^2))$ is $l(s) = (d_2 s_0 - d_1 s)/2d_1 d_2$.

(H_2) implies that $d_1 k^2 - s_0 \geqslant 0$ for all $k \geqslant 1$, that means $D_k = d_1 d_2 k^4 + (d_1 s - d_2 s_0)k^2 - s(s_0 + b) > 0$ for all $k \geqslant 0$. (H_3) implies that $l(s) < 0$, then we can conclude that $D_k > 0$ for all $k \geqslant 0$ since $D_0 > 0$. Clearly, (H_4) implies that $D_k > 0$ for all $k \geqslant 0$. So all roots of (3.3) will have negative real parts under any one of assumptions (H_2), (H_3) and (H_4).

When (H_5) holds, $D(K^2) < 0$, (3.3) has at least one root with positive real part. Hence, (x^*, y^*) is an unstable equilibrium solution of system (3.1). □

The interval I_K is non-trivial only for a finite number of eigenmodes K and apparently $I_K = \emptyset$ if $K^2 \geqslant s_0/d_1$. To guarantee that I_K is non-empty for $K^2 < s_0/d_1$, one can select a large enough

d_2 once d_1 is fixed. When these conditions are met and certain transversality and simplicity conditions are satisfied, a pitchfork bifurcation for the non-constant equilibrium solutions occurs at $s = s_K = \frac{d_2 K^2(s_0 - d_1 K^2)}{d_1 K^2 - (s_0 + b)}$ (see Yi *et al.*, 2009), so for decreasing s, the constant equilibrium (x^*, y^*) loses stability to a non-constant equilibrium before the Hopf bifurcation at $s = s_0 < s_K$. The first such bifurcation point is

$$s_* = \max_{K \in \mathbb{N}} \frac{d_2 K^2(s_0 - d_1 K^2)}{d_1 K^2 - (s_0 + b)}.$$

When $s > s_*$, (x^*, y^*) is locally asymptotically stable for the PDE system (3.1), and it is unstable if $s \leqslant s_*$.

4. Stability of spatially homogeneous periodic orbits

The PDE (3.1) possesses any periodic solution of (2.1) as a spatially homogeneous periodic solution, including the ones from Hopf bifurcation in Theorem 2.1. We can also perform a Hopf bifurcation analysis (Crandall & Rabinowitz, 1977; Hassard *et al.*, 1980) for (3.1) at the same bifurcation point in (2.1), and bifurcating spatially homogeneous periodic solutions exist near $s = s_0$. But the stability of these periodic solutions with respect to (3.1) could be different from that for (2.1). If $\phi(t)$ is an unstable periodic solution of (2.1), then it is clearly also unstable for (3.1); while if $\phi(t)$ is a stable periodic solution of (2.1), it could be unstable for (3.1) because of diffusion.

We use the normal form method and centre manifold theorem in Hassard *et al.* (1980) to study the direction of the Hopf bifurcation. Let L^* be the conjugate operator of L defined as (3.2) in Section 3:

$$L^*(s)\begin{pmatrix} x \\ y \end{pmatrix} := D\begin{pmatrix} x_{rr} \\ y_{rr} \end{pmatrix} + J^*(s)\begin{pmatrix} x \\ y \end{pmatrix}, \tag{4.1}$$

where $J^*(s) := J^\top(s)$, with domain $D_{L^*} = X_{\mathbb{C}}$. Let

$$q = \begin{pmatrix} a_0 \\ b_0 \end{pmatrix} := \begin{pmatrix} 1 \\ \dfrac{-s_0 + i\omega_0}{b} \end{pmatrix}, \quad q^* = \begin{pmatrix} a_0^* \\ b_0^* \end{pmatrix} := \frac{1}{2\pi\omega_0}\begin{pmatrix} \omega_0 + s_0 i \\ bi \end{pmatrix}.$$

It is easy to see that $\langle L^* a, b\rangle = \langle a, Lb\rangle$ for any $a \in D_{L^*}$, $b \in D_L$, and $L(s_0)q = i\omega_0 q$, $L^*(s_0)q^* = -i\omega_0 q^*$, $\langle q^*, q\rangle = 1$, $\langle q^*, \bar{q}\rangle = 0$. Here $\langle a, b\rangle = \int_0^\pi \bar{a}^\top b \, \mathrm{d}r$ denote the inner product in $L^2[(0, \pi)] \times L^2[(0, \pi)]$.

According to Hassard *et al.* (1980), we decompose $X = X^C \oplus X^S$, with $X^C := \{zq + \bar{z}\bar{q} : z \in \mathbb{C}\}$, $X^S := \{w \in X : \langle q^*, w\rangle = 0\}$. For any $(x, y) \in X$, there exists $z \in \mathbb{C}$ and $w = (w_1, w_2) \in X^S$ such that

$$(x, y)^\top = zq + \bar{z}\bar{q} + (w_1, w_2)^\top, \quad z = \langle q^*, (x, y)^\top\rangle.$$

Thus,

$$\begin{aligned} x &= z + \bar{z} + w_1, \\ y &= z\left(\frac{-s_0 + i\omega_0}{b}\right) + \bar{z}\left(\frac{-s_0 + i\omega_0}{b}\right) + w_2. \end{aligned} \tag{4.2}$$

In (z, w) coordinates, system (3.1) becomes

$$\frac{\mathrm{d}z}{\mathrm{d}t} = i\omega_0 z + \langle q^*, \tilde{f}\rangle,$$
$$\frac{\mathrm{d}w}{\mathrm{d}t} = Lw + [\tilde{f} - \langle q^*, \tilde{f}\rangle q - \langle q^*, \tilde{f}\rangle \bar{q}], \tag{4.3}$$

with $\tilde{f} = (f_1, f_2)^\top$, where f_1 and f_2 are defined as (2.3). Straightforward calculations show that

$$\langle q^*, \tilde{f}\rangle = \frac{1}{2\omega_0}[\omega_0 f_1 - (s_0 f_1 + bf_2)i],$$

$$\langle \bar{q^*}, \tilde{f}\rangle = \frac{1}{2\omega_0}[\omega_0 f_1 + (s_0 f_1 + bf_2)i],$$

$$\langle q^*, \tilde{f}\rangle q = \frac{1}{2\omega_0}\begin{pmatrix} \omega_0 f_1 - (s_0 f_1 + bf_2)i \\ [\omega_0 f_1 - (s_0 f_1 + bf_2)i]\,\dfrac{-s_0 + i\omega_0}{b} \end{pmatrix},$$

$$\langle \bar{q^*}, \tilde{f}\rangle \bar{q} = \frac{1}{2\omega_0}\begin{pmatrix} \omega_0 f_1 + (s_0 f_1 + bf_2)i \\ [\omega_0 f_1 + (s_0 f_1 + bf_2)i]\,\dfrac{-s_0 - i\omega_0}{b} \end{pmatrix},$$

$$H(z, \bar{z}, w) := \tilde{f} - \langle q^*, \tilde{f}\rangle q - \langle \bar{q^*}, \tilde{f}\rangle \bar{q} = \begin{pmatrix} 0 \\ 0 \end{pmatrix}.$$

Write $w = (w_{20}/2)z^2 + w_{11}z\bar{z} + (w_{20}/2)\bar{z}^2 + \mathcal{O}(|z|^3)$ for the equation of the centre manifold; we can obtain $(2i\omega_0 - L)\omega_{20} = 0,\ \ (-L)\omega_{11} = 0$ and $\omega_{02} = \bar{w}_{20}$. This implies that $\omega_{20} = \omega_{02} = \omega_{11} = 0$. Thus, the equation on the centre manifold in $z,\ \bar{z}$ coordinates becomes

$$\frac{\mathrm{d}z}{\mathrm{d}t} = i\omega_0 z + \frac{1}{2}g_{20}z^2 + g_{11}z\bar{z} + \frac{1}{2}g_{02}\bar{z}^2 + \frac{1}{2}g_{21}z^2\bar{z} + \mathcal{O}(|z|^4), \tag{4.4}$$

where

$$g_{20} = \langle q^*, (c_0, d_0)^\top\rangle, \quad g_{11} = \langle q^*, (e_0, f_0)^\top\rangle, \quad g_{21} = \langle q^*, (g_0, h_0)^\top\rangle, \tag{4.5}$$

and

$$c_0 := f_{xx}a_0^2 + 2f_{xy}a_0b_0 + f_{yy}b_0^2 = 2A_{20} + 2A_{11}b_0,$$

$$d_0 := g_{xx}a_0^2 + 2g_{xy}a_0b_0 + g_{yy}b_0^2 = 2B_{20} + 2B_{11}b_0 + 2B_{02}b_0^2,$$

$$e_0 := f_{xx}|a_0|^2 + f_{xy}(a_0\bar{b}_0 + \bar{a}_0b_0) + f_{yy}|b_0|^2 = 2A_{20} + A_{11}(\bar{b}_0 + b_0),$$

$$f_0 := g_{xx}|a_0|^2 + g_{xy}(a_0\bar{b}_0 + \bar{a}_0b_0) + g_{yy}|b_0|^2 = 2B_{20} + B_{11}(\bar{b}_0 + b_0) + 2B_{02}|b_0|^2,$$

$$g_0 := f_{xxx}|a_0|^2a_0 + f_{xxy}(2|a_0|^2b_0 + a_0^2\bar{b}_0) + f_{xyy}(2|b_0|^2a_0 + b_0^2\bar{a}_0 + f_{yyy}|b_0|^2b_0)$$
$$= 6A_{30} + 2A_{21}(2b_0 + \bar{b}_0),$$
$$h_0 := g_{xxx}|a_0|^2a_0 + g_{xxy}(2|a_0|^2b_0 + a_0^2\bar{b}_0) + g_{xyy}(2|b_0|^2a_0 + b_0^2\bar{a}_0) + g_{yyy}|b_0|^2b_0$$
$$= 6B_{30} + 2B_{21}(2b_0 + \bar{b}_0) + 2B_{12}(2|b_0|^2 + b_0^2).$$

Here all the partial derivatives are evaluated at the point $(s, x, y) = (s_0, 0, 0)$. Then we obtain

$$g_{20} = \left[A_{20} - \frac{2(s_0+b)}{b}B_{20}\right] - \frac{i}{\omega_0}\left[(A_{20}+A_{11})s_0 + \frac{2s_0^2+3s_0b+b^2}{b}B_{20}\right],$$
$$g_{11} = \left(A_{20} - \frac{s_0}{b}A_{11}\right) - \frac{i}{\omega_0}\left[s_0A_{20} - \frac{s_0^2}{b}A_{11} + (s_0+b)B_{20}\right],$$
$$g_{21} = 3A_{30} - \frac{2}{b}\left[A_{21}s_0 + (s_0+b)B_{12}\right] + \frac{i}{\omega_0}\left[\frac{s_0(2s_0-b)}{b}(A_{21}-B_{12}) - (3A_{30}+6B_{12})s_0 - 3B_{30}\right].$$

According to Hassard *et al.* (1980),

$$c_1(s_0) = \frac{i}{2\omega_0}\left(g_{20}g_{11} - 2|g_{11}|^2 - \frac{1}{3}|g_{02}|^2\right) + \frac{1}{2}g_{21}, \tag{4.6}$$

then

$$\begin{aligned}\mathrm{Re}c_1(s_0) &= \mathrm{Re}\left\{\frac{i}{2\omega_0}\left(g_{20}g_{11} - 2|g_{11}|^2 - \frac{1}{3}|g_{02}|^2\right) + \frac{1}{2}g_{21}\right\}\\ &= \frac{-1}{2\omega_0}(\mathrm{Re}g_{20}\mathrm{Im}g_{11} + \mathrm{Im}g_{20}\mathrm{Re}g_{11}) + \frac{1}{2}\mathrm{Re}g_{21}\\ &= \frac{1}{2\omega_0^2}\Bigg(2s_0A_{20}^2 + \frac{s_0b-2s_0^2}{b}A_{20}A_{11} - \frac{s_0^2}{b}A_{11} + (2s_0+b)A_{20}B_{20}\\ &\quad - s_0(s_0+b)A_{11}B_{20} - \frac{2(s_0+b)^2}{b}B_{20}^2\Bigg) + \frac{3}{2}A_{30} - \frac{s_0}{b}A_{21} - \frac{s_0+b}{b}B_{12}.\end{aligned} \tag{4.7}$$

Comparing the result above with the expression of $a(s_0)$, we find that $\mathrm{Re}c_1(s_0) = \frac{4(s_0+b)}{b}a(s_0)$. Then $\mathrm{Re}c_1(s_0) < 0$ if and only if $a(s_0) < 0$ since $\frac{4(s_0+b)}{b} > 0$. We summarize our analysis results in the following manner.

THEOREM 4.1 Suppose that β, m, s satisfy the same conditions as Theorem 2.2, then system (3.1) undergoes a Hopf bifurcation at (x^*, y^*) when $s = s_0$.

1. The direction of Hopf bifurcation of system (3.1) is the same as that of system (2.1);
2. When $a(s_0) < 0$, the direction of Hopf bifurcation is supercritical, and the bifurcating periodic solutions are asymptotically stable on the centre manifold. Furthermore, they are orbitally asymptotically stable for system (3.1) if and only if one of (H_2), (H_3) and (H_4) holds; they are unstable if (H_5) holds;

3. When $a(s_0) > 0$, the direction of Hopf bifurcation is subcritical, and the bifurcating periodic solutions are unstable on the centre manifold; thus they are unstable for system (3.1).

5. Numerical simulations

In this section, we present some numerical simulations to illustrate our theoretical analysis. The ODE model (2.1) has three parameters: $\beta,\ m,\ s$. We choose parameters:

$$\beta = 0.2, \quad m = 1.5. \tag{5.1}$$

$$\beta = 0.2, \quad m = 4. \tag{5.2}$$

Under (5.1), we have the equilibrium point $(x^*, y^*) \approx (1.0895, 1.0895)$, and the critical point $s_0 \approx 0.1899$ and $a(s_0) \approx -0.0370 < 0$. By Theorem 2.2, the equilibrium is asymptotically stable when $s > s_0$; a Hopf bifurcation occurs at $s = s_0$, the bifurcating periodic solutions occur when $s < s_0$ and the bifurcating periodic solutions are asymptotically stable (Fig. 3).

Under (5.2), the equilibrium point $(x^*, y^*) \approx (0.3066, 0.3066)$, the critical point $s_0 \approx 0.1590$ and $a(s_0) \approx 0.0650 > 0$. By Theorem 2.2, the equilibrium is asymptotically stable when $s > s_0$; the bifurcating periodic solutions occur when $s > s_0$ and the bifurcating periodic solutions are unstable. These are shown in Fig. 4.

The PDE model has five parameters: $\beta,\ m,\ s,\ d_1,\ d_2$. We choose three sets of parameters as follows:

$$\beta = 0.2,\ m = 1.5,\ d_1 = 0.008,\ d_2 = 1,\ s = 0.25, \tag{5.3}$$

$$\beta = 0.2,\ m = 1.5,\ d_1 = 1,\ d_2 = 1,\ s = 0.3, \tag{5.4}$$

$$\beta = 0.2,\ m = 1.5,\ d_1 = 1,\ d_2 = 1,\ s = 0.15, \tag{5.5}$$

$$\beta = 0.2,\ m = 1.5,\ d_1 = 0.008,\ d_2 = 1,\ s = 0.15. \tag{5.6}$$

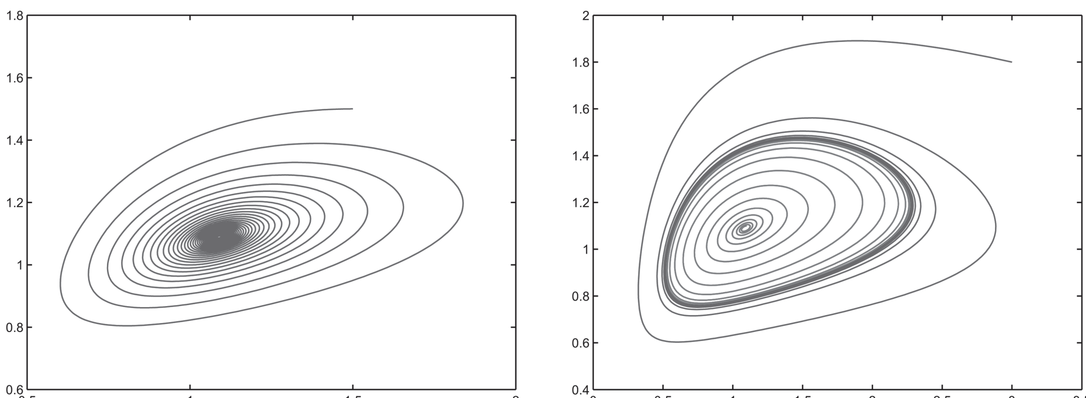

FIG. 3. Phase portraits of (2.1) with parameters in (5.1). Left: $s = 0.2 > s_0$, the positive equilibrium is asymptotically stable (initial condition is $(x_0, y_0) = (1.5, 1.5)$); right: $s = 0.15 < s_0$, the bifurcating periodic orbit is stable (initial condition $(x_0, y_0) = (1.1, 1.1)$ and $(x_0, y_0) = (3, 1.8)$).

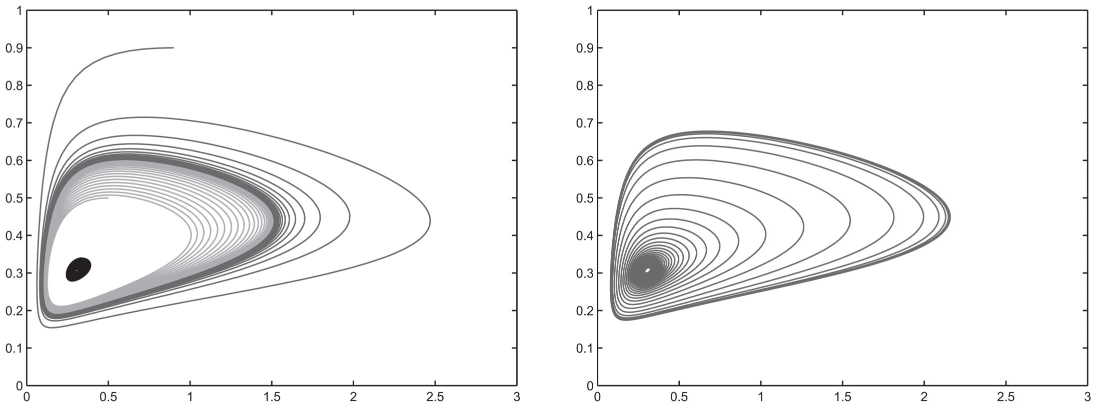

FIG. 4. Phase portraits of (2.1) with parameters in (5.2). Left: $s = 0.162 > s_0$, the positive equilibrium is asymptotically stable, and the bifurcating periodic solutions are unstable; right: $s = 0.15 < s_0$, the positive equilibrium is unstable, there exists a stable periodic orbit (initial condition $(x_0, y_0) = (0.34, 0.34)$, $(x_0, y_0) = (0.5, 0.5)$ and $(x_0, y_0) = (0.9, 0.9)$ in the left panel and $(x_0, y_0) = (0.3, 0.3)$ in the right panel).

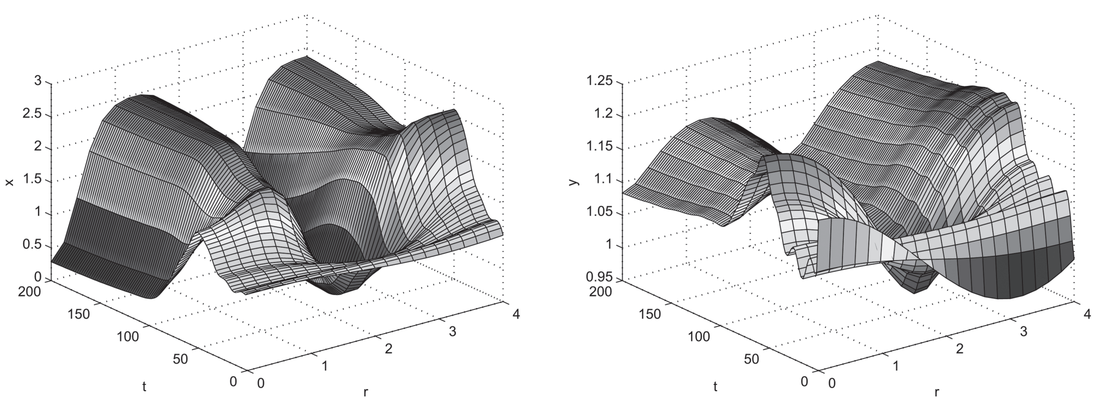

FIG. 5. Numerical simulations of the Turing instability of the equilibrium solution of system (3.1) under (5.3). The solution appears to converge to a non-homogeneous steady state (initial condition $(x_0, y_0) = (0.1 \cos r + 1.08, 0.1 \cos r + 1.08)$). Left: component x; right: component y.

Under (5.3), $s_0 \approx 0.1899$ and $s = 0.25 \in T_b$, i.e., (H_5) holds for $K = 1, 2, 3, 4$. By Theorem 3.1, the homogeneous equilibrium solution $(x^*, y^*) \approx (1.0895, 1.0895)$ of system (3.1) is unstable. Figure 5 shows the Turing instability of the equilibrium solution.

Under (5.4), $s_0 \approx 0.1899$, $\mathrm{Re}\, c_1(s_0) \approx -0.0901 < 0$ and (H_2) holds. By Theorem 3.1, the homogeneous equilibrium solution (x^*, y^*) of system (3.1) is locally asymptotically stable (see Fig. 6).

Under (5.5), $s_0 \approx 0.1899$, $\mathrm{Re}\, c_1(s_0) \approx -0.0901 < 0$ and (H_2) holds; the choice of s satisfies $s < s_0$. By Theorem 4.1, Hopf bifurcation occurs at $s = s_0$, the bifurcating periodic orbits exist for $s < s_0$, which are orbitally asymptotically stable. This is shown in Fig. 7.

Under (5.6), $s_0 \approx 0.1899$, $\mathrm{Re}\, c_1(s_0) \approx -0.0901 < 0$ and (H_5) holds for $K = 3$ in Theorem 3.1; the choice of s satisfies $s < s_0$. By Theorems 4.1 and 3.1, the bifurcating periodic orbits exist for $s < s_0$, which are Turing unstable. In Fig. 8, we can see the solution from $(x_0, y_0) = (0.1 \cos r +$

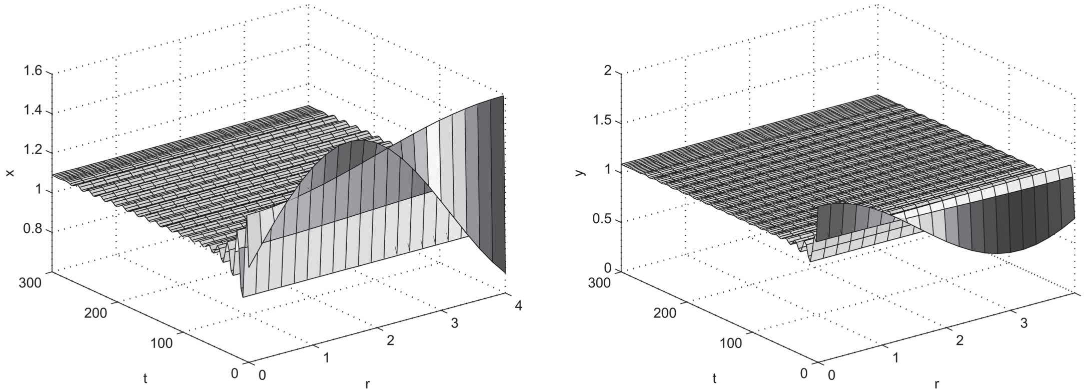

FIG. 6. Numerical simulations of the stable equilibrium solution of system (3.1) under (5.4). The solution appears to converge to a homogeneous steady state (initial condition $(x_0, y_0) = (0.5 \sin r + 1.08, 0.5 \cos r + 1.08)$). Left: component x; right: component y.

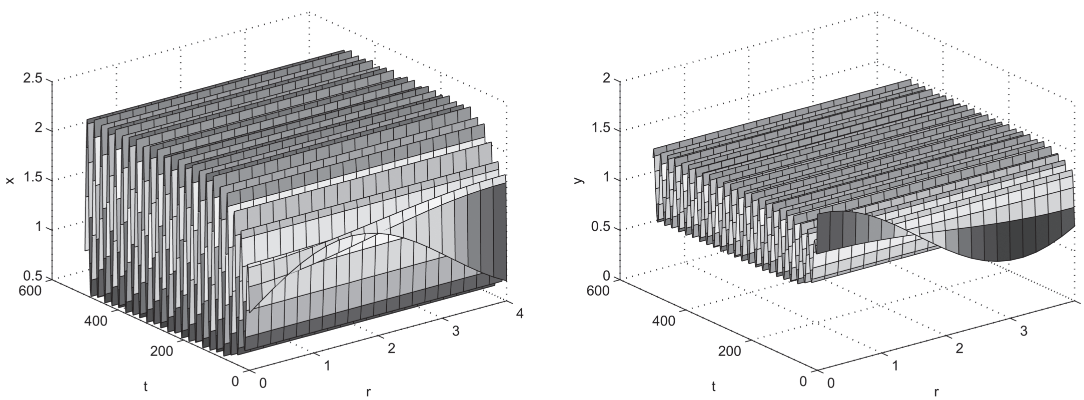

FIG. 7. Numerical simulations of the stable periodic solution of system (3.1) under (5.5) and $s = 0.15 < s_0$. The solution appears to converge to a homogeneous periodic orbit (initial condition $(x_0, y_0) = (0.5 \sin r + 1.08, 0.5 \cos r + 1.08)$). Left: component x; right: component y.

$1.08, 0.1 \cos r + 1.08)$ is attracted by a positive non-constant stable equilibrium. This verifies the results previously proved in Peng & Wang (2005).

6. Conclusions

A rigorous investigation of the dynamics of an R-D Holling–Tanner model subject to Neumann boundary condition is attempted, and the main purpose of this article is to identify the parameter ranges of stability and instability of spatially homogeneous equilibrium solutions and bifurcating periodic orbits. We summarize our investigation on the bifurcation diagram of the parameters m and s (see Fig. 9).

For the ODE system (2.1), a curve L_2: $s = s_0$ separates the stable region (above L_2) and the unstable region (below L_2); a Hopf bifurcation occurs when the parameter crosses L_2 transversally, and at least one periodic orbit exists for parameter values below L_2. A vertical line L_a: $\mathrm{Re}c_1(s_0) = a(s_0) = 0$ separates the region of supercritical Hopf bifurcations (on the left of L_a) and subcritical ones (on the

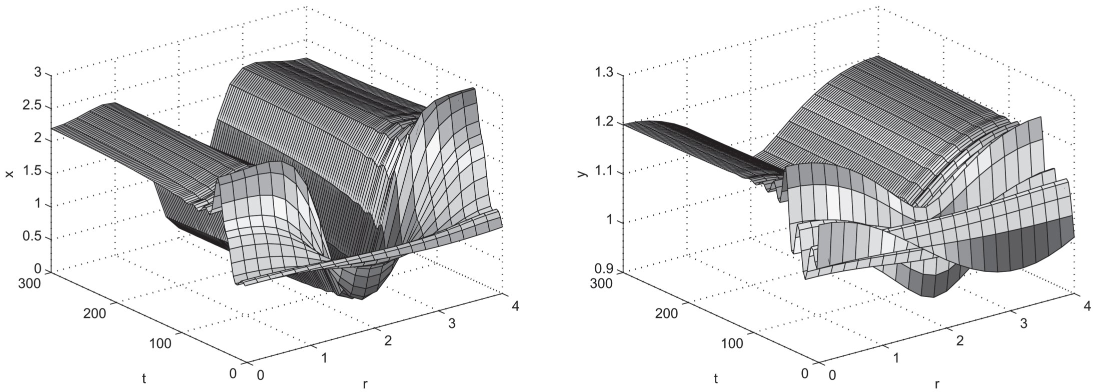

FIG. 8. Numerical simulations of the Turing instability of the bifurcating periodic orbit and the existence of positive non-homogeneous steady states of system (3.1) under (5.6). The solution appears to converge to a non-homogeneous steady state (initial condition $(x_0, y_0) = (0.1\cos r + 1.08, 0.1\cos r + 1.08)$). Left: component x; right: component y.

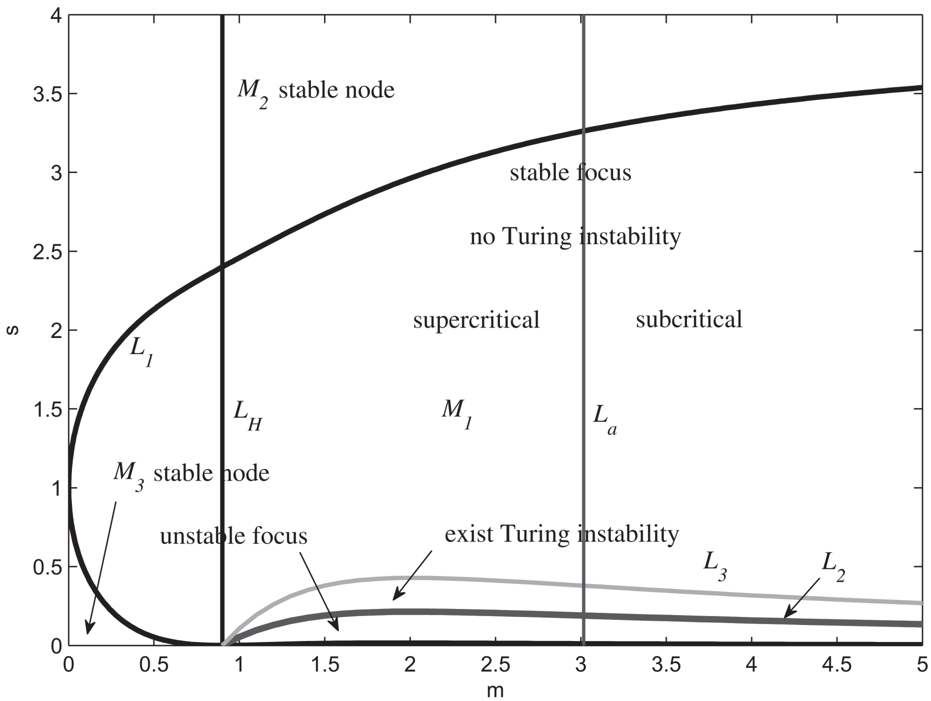

FIG. 9. Bifurcation diagram in (m, s) parameter space. Here we choose $\beta = 0.2$ and $d_2/d_1 = 2$. L_1 is the curve $(s_0 + s)^2 + 4bs = 0$ where the Jacobian $J(s)$ has repeated eigenvalues, and L_1 divides the first quadrant into three parts: M_1 (stable/unstable focus), M_2 (stable node) and M_3 (stable node). The ODE Hopf bifurcation curve L_2 is $s = s_0$, above (below) which (x^*, y^*) is a stable (unstable) focus for the ODE system. The curve L_3 is $s = d_2 s_0/d_1$, and between L_2 and L_3, Turing instability could occur for (x^*, y^*) for the PDE system. The vertical line L_H is $s_0 = 0$ ($m = 0.9$ here), and on the left side of L_H (x^*, y^*) is globally asymptotically stable with respect to the ODE system. The vertical L_a is $\mathrm{Re}\,c_1(s_0) = a(s_0) = 0$ ($m = 3.016$ here), and on the left (right) side of L_a the Hopf bifurcation at $s = s_0$ is supercritical (subcritical).

right of L_a). Hence, on the right side of L_a, (2.1) may have two periodic orbits for $s \in (s_0, s_0 + \epsilon)$. A further vertical line L_H: $s_0 = 0$ identifies a parameter region (on the left side of L_H) where the coexistence equilibrium (x^*, y^*) is globally asymptotically stable with respect to the ODE dynamics (2.1). On the right side of L_H (and above L_2), (x^*, y^*) is locally asymptotically stable for (2.1). Finally, a curve L_1: $(s_0 + s)^2 + 4bs = 0$ separates the region where (x^*, y^*) is a focus or node.

The equilibrium solutions and periodic solutions of the ODE system (2.1) are spatially homogeneous solutions of the R-D system (3.1). Hence, the ODE dynamics of (2.1) is a subdynamics of the one of (3.1). The direction of Hopf bifurcation of system (3.1) st $s = s_0$ is also same as that of system (2.1). But the stability of the solutions can change because of the effect of diffusion. If the parameter value (m, s) is chosen above curve L_3, then the stability of the coexistence equilibrium (x^*, y^*) with respect to the PDE (3.1) is the same as that of (2.1), and there will be no Turing instability of the spatially homogeneous equilibrium. But such a diffusion-induced instability can occur for parameter values chosen between the curves L_2 and L_3. The Turing bifurcations of spatially non-homogeneous equilibrium solutions that occurred between L_2 and L_3 and further Hopf bifurcations of spatially non-homogeneous periodic orbits that occurred below L_2 will be of interest for further investigation.

Funding

National Natural Science Foundation of China; Heilongjiang Provincial Natural Science Foundation (A200806); Program of Excellent Team and Science Research Foundation in Harbin Institute of Technology.

References

Chen, S., Shi, J. & Wei, J. (2010) Global stability and Hopf bifurcation in a delayed diffusive Leslie-Gower predator-prey system (submitted for publication).

Crandall, M. G. & Rabinowitz, P. H. (1977) The Hopf bifurcation theorem in infinite dimensions. *Arch. Ration. Mech. Anal.*, **67**, 53–72.

Du, Y. & Hsu, S. B. (2004) A diffusive predator-prey model in heterogeneous environment. *J. Differ. Equ.*, **203**, 331–364.

Gasull, A., Kooij, R. E. & Torrgrosa, J. (1997) Limit cycles in the Holling-Tanner model. *Publ.* Mat., **41**, 149–167.

Guckenheimer, J. & Holmes, P. J. (1983) *Nonlinear Oscillations, Dynamical Systems, and Bifurcation of Vector Fields*. New York: Springer.

Han, W. & Bao, Z. (2009) Hopf bifurcation analysis of a reaction-diffusion Sel'kov system. *J. Math. Anal. Appl.*, **356**, 633–641.

Hassard, B. D., Kazarinoff, N. & Wan, Y.-H. (1980) *Theory and Applications of Hopf Bifurcation*. Cambridge: Cambridge University Press.

Hsu, S. B. & Huang, T. W. (1995) Global stability for a class of predator-prey system. *SIAM J. Appl. Math.*, **55**, 763–783.

Hsu, S. B. & Huang, T. W. (1998) Uniqueness of limit cycles for a predator–prey system of Holling and Leslie type. *Can. Appl. Math. Quart.*, **6**, 91–117.

Hsu, S. B. & Huang, T. W. (1999) Hopf bifurcation analysis for a predator-prey system of Holling and Leslie type. *Taiwanese J. Math.*, **3**, 35–53.

Liu, J., Yi, F. & Wei, J. (2010) Multiple bifurcation analysis and spatiotemporal patterns in a 1-D Gierer-Meinhardt model of morphogenesis. *Int. J. Bifurcation Chaos*, **20**, 1007–1025.

Marsden, J. E. & McCracken, M. (1976) *The Hopf Bifurcation and its Applications*. New York: Springer.

MAY, R. M. (1973) *Stability and Complexity in Model Ecosystems*. Princeton, NJ: Princeton University Press.

MURRAY, J. D. (2002) *Mathematical Biology I. An Introduction,* 3rd edn. Berlin: Springer, pp. 88–94.

PENG, R. & WANG, M. X. (2005) Positive steady-states of the Holling-Tanner prey-predator model with diffusion. *Proc. Roy. Soc. Edin.*, **135A**, 149–164.

PENG, R. & WANG, M. X. (2007) Global stability of the equilibrium of a diffusive Holling-Tanner prey-predator model. *Appl. Math. Lett.*, **20**, 664–670.

RUAN, S. G. (1998) Diffusion-driven instability in the Gierer-Meinhardt model of morphogenesis. *Nat. Resour. Model.*, **11**, 131–142.

SHI, J. (2009) Bifurcation in infinite dimensional spaces and applications in spational biological and chemical models. *Front. Math. China*, **4**, 407–424.

TANNER, J. T. (1975) The stability and intrinsic growth rates of prey and predator populations. *Ecology*, **56**, 855–867.

TURING, A. M. (1952) The chemical basis of morphogenesis. *Philos. Trans. R. Soc. Lond. B*, **237**, 37–72.

WIGGINS, S. (1990) *Introduction to Applied Nonlinear Dynamical System and Chaos*. New York: Springer.

YI, F., LIU, J. & WEI, J. (2010) Spatiotemporal pattern formation and multiple bifurcations in a diffusive bimolecular model. *Nonlinear Anal. B Real World Appl.*, **11**, 3770–3781.

YI, F., WEI, J. & SHI, J. (2008) Diffusion-driven instability and bifurcation in the Lengyel-Epstein system. *Nonlinear Anal. B Real World Appl.*, **9**, 1038–1051.

YI, F., WEI, J. & SHI, J. (2009a) Bifurcation and spatiotemporal patterns in a homogeneous diffusive predator-prey system. *J. Differ. Equ.*, **246**, 1944–1977.

YI, F., WEI, J. & SHI, J. (2009b) Global asymptotical behavior of the Lengyel-Epstein system. *Appl. Math. Lett.*, **22**, 52–55.